Catalysis Today xxx (xxxx) xxx–xxx

Contents lists available at ScienceDirect

Catalysis Today

journal homepage: www.elsevier.com/locate/cattod

Post-modified FAU zeolites as efficient catalysts for the synthesis of coumarins

O. Zaitceva[a], B. Louis[b,*], V. Beneteau[a], P. Pale[a], S. Shanmugam[c], E.I. Evstigneyev[d], A.V. Vasiliev[d,e,**]

[a] Institut de Chimie, UMR 7177, CNRS and Université de Strasbourg, Strasbourg, 4 rue Blaise Pascal, 67000 Strasbourg, France
[b] ICPEES, Institut de Chimie et Procédés pour l'Energie l'Environnement et la Sante, Energy and Fuels for a Sustainable Environment Team, UMR 7515 CNRS, Université de Strasbourg, 25 rue Becquerel, F-67087, Strasbourg Cedex 2, France
[c] Department of Energy Science & Engineering, Daegu Gyeongbuk Institute of Science and Technology (DGIST), 50-1 Sang-Ri, Hyeongpung-Myeon, Dalseong-gun, Daegu, 711-873, Republic of Korea
[d] Saint Petersburg State Forest Technical University, 5 Institutskii per., 194021, Saint Petersburg, Russian Federation
[e] Saint Petersburg State University, 7/9 Universitetskaya Nab., 199034, Saint Petersburg, Russian Federation

ARTICLE INFO

Keywords:
Zeolite
FAU
Desilication
Lignin
Coumarins
Biorefinery

ABSTRACT

Herein, the effect of various treatments subjected to FAU zeolites to introduce mesoporosity has been examined on their efficiency as catalyst in the cyclisation of *O*-aryl 3-arylpropynoic acid ester to its corresponding coumarin.

The addition of bio-sourced lignin residues in the alkaline desilication treatment induced the generation of supplementary mesoporosity, thus offering an optimal *micro-* and *mesopores* combination with respect to targeted activity and selectivity.

The so-called bio-sourced secondary template (BSST) concept in the design of zeolite-based catalysts could be assessed. The use of renewable wood feedstocks can therefore be a valuable strategy for the zeolite post-modification, thus for the design of porous zeolite catalysts.

1. Introduction

Zeolites are microporous crystalline aluminosilicates built by vertex-sharing aluminate and silicate tetrahedra [1]. Zeolites have found kaleidoscopic applications during the past sixty years. Currently, more than 230 different zeolite topologies are known with roughly 15 being used in industry. However, five structures belong to the so-called 'big five' including MOR, BEA, FER, MFI and FAU zeolites which are extensively used in industry. Among them, MFI and FAU are prominent materials applied in catalysis thanks to their acid strength, high hydrothermal stability, ability to induce shape selectivity and also the reproducibility (and low cost) of their synthesis procedures and post-modifications [2].

Zeolites are often associated to slow mass transfer within their microporous architecture with channels and cages of molecular size (< 1 nm). This may strongly impact the catalyst lifetime, its performance as well as sometimes loss in selectivity due to undesired by-products formation. Numerous studies were focused on the development of strategies to improve transport properties, which are usually classified in three categories: (i) smaller crystal size; (ii) larger pore zeolites (2 nm); (iii) formation of mesopores along with the microporous network. The first approach raises several drawbacks concerning the limited technology available for the synthesis and handling of nanocrystals [3]. Materials with larger pores, although improving the mass transport, often penalize the catalytic activity, stability and selectivity properties of microporous structures [4,5]. The third strategy has been widely selected to design materials with hierarchical porosities, inducing an enhanced diffusion of reactants and products, hence raising the conversion in the cracking of large molecules and the catalyst lifetime [6–10].

In parallel to those aforementioned approaches, Rimer and coworkers have thoroughly investigated the impact of zeolite growth modifiers (ZGMs) as polyamines, sugars, or proteins on the construction of crystal sub-units [11–14]. They were able to alter the crystal growth and therefore tailor the size and morphology of the crystals [11–14].

Inspired by those seminal studies, we have developed the so-called

* Corresponding author.
** Corresponding author at: Saint Petersburg State Forest Technical University, 5 Institutskii per., 194021, Saint Petersburg, Russian Federation.
E-mail addresses: blouis@unistra.fr (B. Louis), aleksvasil@mail.ru (A.V. Vasiliev).

https://doi.org/10.1016/j.cattod.2020.06.081
Received 3 April 2020; Received in revised form 9 June 2020; Accepted 29 June 2020

Bio-Sourced Secondary Template (BSST) concept, involving biomass residues in the synthesis of several zeolite topologies [15–17]. Despite the lack of understanding the exact nature of organic molecules involved in the interactions with inorganic precursors, sophisticated crystal assemblies generating inter-crystalline meso- or macroporosities were obtained [18–20]. However, it is well-admitted that the presence of intra-crystalline mesoporosity is preferred to achieve better catalyst performances [21,22].

In the present contribution, a destructive desilication strategy has been undertaken to introduce mesoporosity in FAU zeolite crystals while adding lignin residues to the alkaline medium. Although structurally quite complex, lignin has been chosen due to its large availability. For instance, in Russia, nearly 95 million tons are stored as a waste after bio-ethanol production in bio-refineries [23]. As-obtained FAU zeolites containing micro- and mesoporosities were then tested in the synthesis of coumarins which are valuable building blocks in organic synthesis.

2. Experimental section

2.1. Procedures for lignin modification

The lignin originates from the Kirov plant (city of Kirov, Russia). The chemical composition and properties of industrial acid hydrolysed lignin (HL) as well as its oxidized hydrolysed form (OHL) are given in Table 1. The procedure of HL oxidation into OHL has been reported by Evstigneyev et al. [24].

The methods used for determining the composition of HL and OHL were as follows: Klason lignin (insoluble residue) and acid-soluble lignin were determined according to the methods reviewed by Dence [25]. Carbohydrates contents were determined by photocolorimetry using the phenol – sulfuric acid method [26]. The quantity of methoxy groups were determined by the reaction between lignins and hydroiodic acid [27]. Carboxyl groups were determined by an ion-exchange method according to Wilson [28], which was slightly modified for lignin analysis [29]. Phenolic hydroxyl groups were determined by Mänsson's aminolysis method [30]. Carbonyl groups were determined by a reaction with hydroxylamine hydrochloride [27]. The total ash content was obtained by the TAPPI method [27].

An alkaline solution of OHL was prepared according to the following protocol: OHL dissolution was carried out in a 1 L round-bottomed three-necked flask equipped with a thermometer, a propeller stirrer and a reflux condenser, on a mantle heater. The alkali solution (3.6 g of NaOH in 0.5 L of water) was placed in a flask and through the side outlet, 20 g of OHL were added in small portions under vigorous stirring. The temperature in the flask was then raised to 85 °C and stirring was continued for 1 h. The solution was then cooled and its pH was measured, being 9.5. Hence, 0.5 L of OHL solution with a concentration of 40 g/L was obtained.

2.2. FAU zeolite post-modifications

Pristine FAU zeolite provided by Zeochem (Zeoflair 200, Uetikon, Switzerland) was used in its sodium form NaY. A cationic exchange with a 1 M aqueous solution of ammonium nitrate (Fluka) was performed three times at 65 °C to get the NH_4-Y form. In order to obtained acidic HY zeolite, a calcination at 550 °C in air during 15 h was performed in a muffle furnace.

Table 1
Characterisation of hydrolysed lignin (HL) and oxidized hydrolysed lignin (OHL), content, mass %.

Lignin	Klason lignin	Carbohydrates	OMe	COOH	OH_{phen}	C = O	Ash
HL	89.52 (0.28)[a]	6.79	11.97	4.49	3.00	4.15	3.37
OHL	87.35 (2.66)[a]	5.07	5.52	10.28	2.07	5.13	0.96

Note: [a] content of acid-soluble lignin is given under brackets.

Table 2
Chemical composition and textural properties of pristine and post-modified zeolites.

Sample	Si/Al	S BET [m^2/g]	S micro [m^2/g]	S meso [m^2/g]	Pore Volume [cm^3/g]	V micro [cm^3/g]	V meso [cm^3/g]	D meso [nm]
NaY	37	653	541	112	0.31	0.26	0.05	2
EFAI-USY	36	872	726	146	0.44	0.35	0.09	11
No-EFAI-USY	57	667	528	139	0.31	0.25	0.06	11
D14	40	861	677	184	0.44	0.33	0.11	10
A4	18	402	146	256	0.31	0.07	0.24	15
A13	15	463	198	265	0.46	0.10	0.36	22

2.2.1. Steaming – EDTA treatment

Pristine acidic HY zeolite was dealuminated by steaming as follows: 1 g HY was placed in a fixed-bed reactor. The catalyst was heated up to 550 °C (10°/min ramp) under nitrogen flow (45 mL/min). A vapor pressure of 85 kPa was then fed to the catalyst (under nitrogen flow) during 24 h. This sample was named EFAl-USY.

The latter EFAl-USY sample (0.5 g) was then subjected to a treatment with 30 mL of EDTA solution (ethylenediaminetetraacetic acid, 0.25 M) under stirring at 60 °C during 5 h. After the sample was filtered and dried in an oven at 150 °C during 15 h. This treatment aimed in the complexation and removal of extra-framework Al species generated during the steaming treatment in EFAl-USY. This sample is named No-EFAl-USY.

2.2.2. Desilication

0.5 g of parent HY zeolite was desilicated in a 20 mL aqueous solution composed by 0.2 M NaOH and 0.2 M TBAOH (1:1 vol/vol) at room temperature during 30 min under stirring. After, the sample was filtered on a Nylon membrane, dried and calcined at 550 °C for 15 h under air atmosphere in a muffle furnace. This sample was named D14.

2.2.3. Destructive-constructive strategy using lignin

A conventional desilication strategy in alkaline medium was undertaken and combined with a potential meso-structuration mediated by lignin residues, according to our recently reported BSST concept [15]. 0.5 g of H-form parent zeolite was mixed with a 0.1 M solution of TEAOH for 5 min up to 96 h. Afterward, 0.1 g of HL or OHL residues were added to the mixture and allowed stirring during 10 min. The solution was poured in a Teflon-lined stainless-steel autoclave (70 mL volume) and heated to 150 °C. The hydrothermal treatment was performed during 15 h. After cooling to room temperature, the solid was filtered and calcined under air at 550 °C during 15 h. The sample left during 5 min in the strong alkaline solution, prior to hydrothermal treatment, was named A4. Besides, the sample placed during 96 h in TEAOH solution was named A13. The synthesis yields after autoclaving were 59 and 57 %, respectively. It is worthy to mention here that whatever the origin of added lignin residues, the same yields could be obtained.

2.3. Characterisation

X-ray diffraction patterns (XRD) were recorded on a Bruker D8 Advance diffractometer, with a Ni detector side filtered Cu Kα radiation (1.5406 Å) over a 5 – 60° 2θ range and a position sensitive detector using a step size of 0.02° and a step time of 2 s.

Scanning Electron Microscopy (SEM) micrographs were acquired on a Zeiss Gemini SEM 500 microscope working at 9 kV accelerating

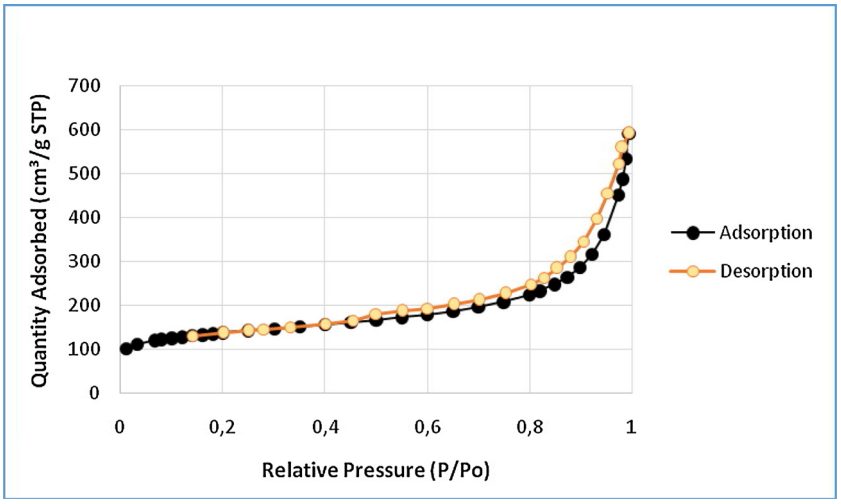

Fig. 1. Nitrogen adsorption-desorption isotherm for desilicated A13 sample.

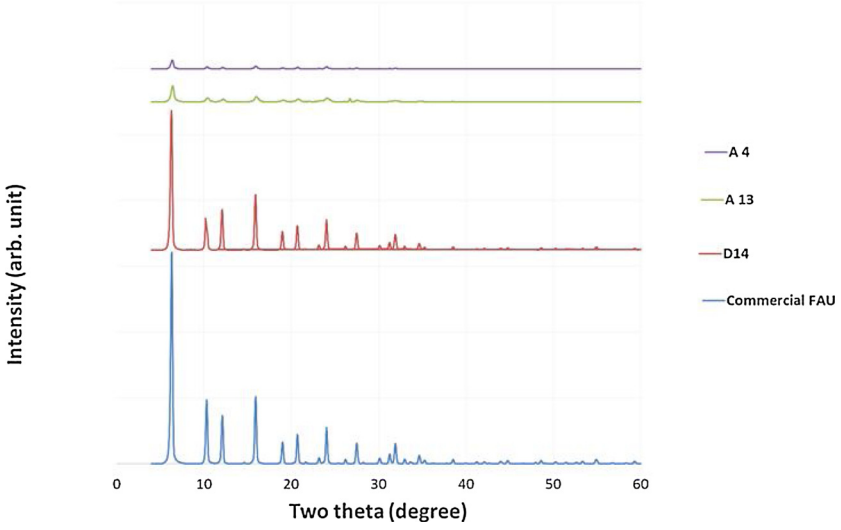

Fig. 2. XRD patterns of pristine FAU zeolite and its desilicated counterparts.

voltage. The Si/Al ratios (SAR) of the zeolites were determined by X-ray fluorescence using a SPECTRO XEPOS spectrometer (He gas atmosphere) equipped with a 50-Watt end-window X-ray tube to excite the samples.

For TEM investigations, the samples were dispersed in ethanol, sonicated for few seconds and drop-deposited on a copper TEM grid with a holey carbon film. HRTEM images and elemental composition of the materials were acquired over a Hitachi HF-3300 kV instrument.

The basic texture characteristics involving the apparent BET surface area S_{BET}, the micropore surface area S_{micro} and the micropore volume $V\mu$ were evaluated from N_2 physical adsorption-desorption isotherms measured at 77 K by means of ASAP2020 M instrument (Micromeritics, USA). The high precision of pressure measurements was achieved by the use of a low-pressure transducer with the capacity of 0.1 Torr. The specific surface area, S_{BET}, was evaluated from the nitrogen adsorption isotherm in the range of relative pressure $p/p_0 = 0.05–0.25$ (p is the adsorbate pressure and p_0 is the adsorbate vapor pressure at the measuring temperature) using the standard Brunauer–Emmett–Teller (BET) procedure.

2.4. Synthesis of coumarins

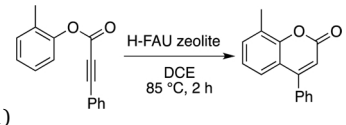

(1)

In a sealed tube (with a screw cap) 2-methylphenyl 3-phenylpropynoate (45 mg, 1 eq.) was added, along with H-FAU zeolites (5 eq. mmol H^+/g) and 2 mL of 1,2-dichloroethane (DCE). The reaction was performed at 85 °C during 2 h under vigorous stirring (Eq. 1). Then, the mixture was filtered over a nylon membrane (0.2 µm) and thoroughly washed with 5 mL of DCE. The zeolite was collected from the filter in a 50 mL round-bottomed flask and stirred with 20 mL of methanol at room temperature for 2 h. After, the two filtrates were combined and the solvents were removed under reduced pressure. The resulting 8-methyl-4-phenyl-*2H*-chromen-2-one product was purified by column chromatography on silica gel, eluents – cyclohexane : ethyl acetate (90 : 10). Equation 1 summarizes the reagents and the conditions used for this reaction.

The quantification of both the conversion of *O*-aryl ester of 3-arylpropynoic acid and the yield in 8-methyl-4-phenyl-*2H*-chromen-2-one coumarin was performed by ^{1}H NMR using internal standard recorded on a Bruker Avance 400 instrument.

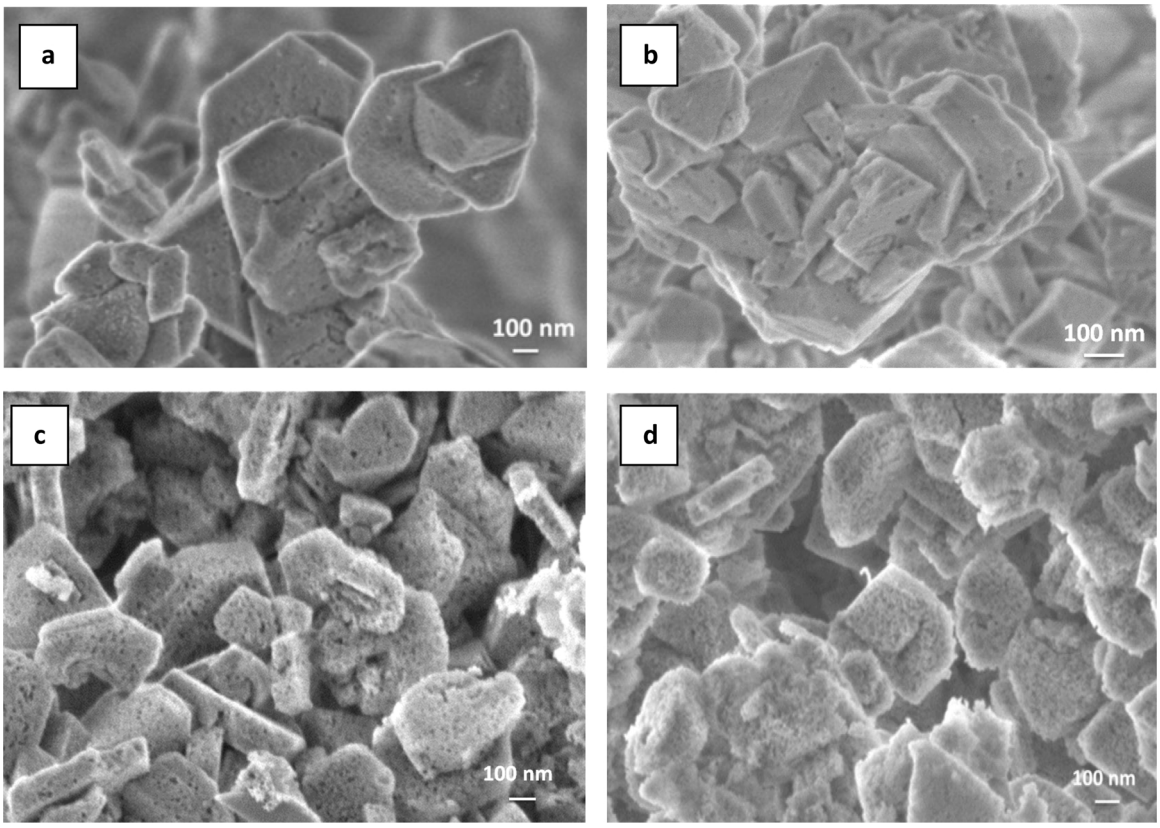

Fig. 3. SEM images of a) parent HY; b) desilicated D14; c) A4; d) A13 sample.

3. Results

3.1. Characterisation

Table 2 presents the textural properties of pristine and all post-modified FAU zeolites. It is noteworthy that steaming treatment did not lead to changes in the Si/Al ratio. Indeed, steaming is known to allow the migration of Al atoms from the framework to extra-framework positions without altering the global Al-content. In contrast, the complexation of EFAl species with EDTA led to raise Si/Al from 36 to 57 for EFAl-USY and No-EFAl-USY, respectively. Those observations are in line with former studies from Bokhoven and co-workers [31]. Besides, mesoporous surface areas as well as the size of the mesopores have been enhanced. However, the desilication in alkaline medium (D14 sample) seems more efficient for the generation of intra-crystalline mesoporosity, as '*a priori*' expected [8,9,32]. The last two samples, A4 and A13, prepared via a destructive / re-constructive strategy using lignins led to a stark decrease in the SAR (18 and 15 for A4 and A13, respectively), suggesting an extensive desilication during the hydrothermal treatment in alkaline medium. Likewise, this harsh treatment led to a drastic increase in their mesoporous specific areas and volumes, at the expense of their microporous textural properties. Fig. 1 shows the N_2 adsorption-desorption isotherm for the most desilicated A13 sample. A typical type IV profile with a hysteresis loop could be observed, thus confirming the presence of mesoporosity. It is important to add here that the use of either HL or OHL sources led to the same results.

According to the data taken from Table 1, the crystallinity of the samples has also been compared to evaluate the impact of the different chemical treatments. Fig. 2 shows the XRD patterns of those post-treated samples.

It can be observed that D14 does not exhibit any substantial loss in crystallinity. This is in line with the textural properties found in Table 1, where no loss in microporosity could be assessed. In stark contrast, A4 and A13 samples suffered a drastic decrease in their crystallinities (Fig. 2). Though the main diffractions of the FAU structure can still be observed, their intensities remain by far lower than those from HY or D14 samples. Based on the observations taken from Table 1, it seems that a partial amorphisation of the zeolite structure occurred during the alkaline and hydrothermal treatment. It is important to mention here that both HL and OHL lignin sources led to the same results.

Fig. 3 shows the SEM images of the different samples. While the crystal size (between 300 – 600 nm) and pyramidal morphology did not change after the different desilication treatments, the presence of numerous mesopores can be observed in post-treated samples (Fig. 3b–d). The extent of these networks of mesopores can be particularly detected in A4 and A13 samples.

A closer look to the porosity organization by TEM analysis (Fig. 4) further confirms the SEM observations. A regular array of micropores having roughly 1.4 nm in width could be assessed for parent FAU zeolite. The 2 nm mesopores detected by nitrogen adsorption measurements (Table 1) usually correspond to intercrystalline porosity [33]. Fig. 4b and c confirm the presence of numerous mesopores in A4 and A13 samples, respectively. Though being rather disorganized in terms of orientation, their size distribution is rather narrow and found between 15 – 25 nm for both samples. Again, these values are in line with those obtained by textural properties analyses (Table 1). It is also noteworthy that the array of micropores almost completely vanished after those two harsh post-treatments.

3.2. Synthesis of coumarins

Coumarins, also named *2H*-chromen-2-ones or *2H*-1-benzopyran-2-ones, encompass a large number of natural products, isolated from a large range of plant sources as well as micro-organisms and animals. Coumarins exhibit a broad range of activity that make their core a

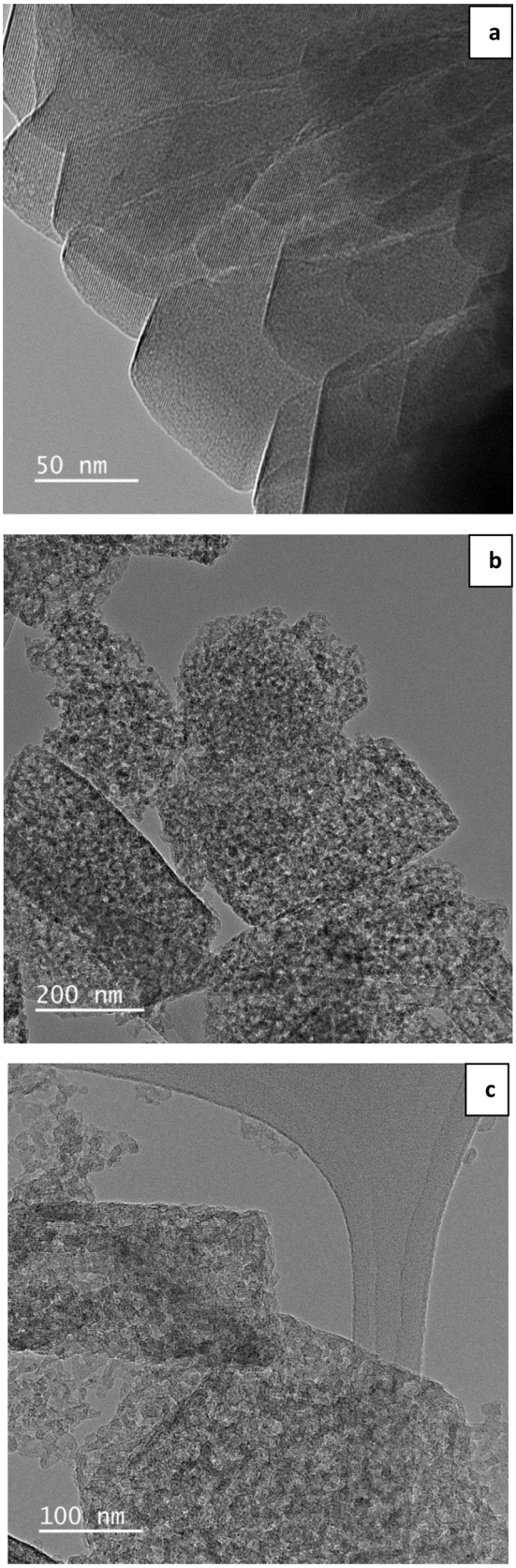

Fig. 4. TEM images of a) HY zeolite; b) A4; c) A13 sample.

privileged scaffold found in several pharmaceutical, agrochemical and cosmetic compounds [34]. *O*-aryl ester of 3-arylpropynoic acid was tentatively converted into its corresponding coumarin as described in Section 2.4 (Eq. 1). The ester 2-methylphenyl 3-phenylpropynoate was selected as a model for the present study. More examples and experimental details can also be found in our former contribution [35].

Table 3 presents the conversion of 2-methylphenyl 3-phenylpropynoate and the selectivity towards targeted 8-methyl-4-phenyl-*2H*-chromen-2-one coumarin. It appears that the highest activity was achieved over A4 catalyst with almost twice higher conversion than pristine HY zeolite, 56 *versus* 30 %. It seems therefore that the post-treatment, which allowed converting part of the FAU microstructure into barely organized mesopores of roughly the same size, increases activity and provides an optimal catalyst for this reaction.

The comparison of the latter results, gained with A4 and A13 samples, suggests that the presence of mesopores is required to improve the quantity of *O*-aryl ester of 3-arylpropynoic acid converted, but not too much. Indeed, A13 exhibits a larger volume of mesopores than A4 (0.36 vs 0.24 cm^3/g) but also the largest mesopore diameter (22 vs 15 nm), while acting as the worst catalyst of the examined series. It is worth to note that the second-best result (47 % conversion) was achieved with sample D14, which also exhibits a large mesoporous volume (0.11 cm^3/g) with an important mesoporous diameter (10 nm).

These observations and data guided us to set an 'optimum', thus being able to maximize the degree of conversion at an appreciable selectivity towards coumarin. Fig. 5 presents the correlation between the degree of *O*-aryl ester conversion and the mesoporous volume present in the different zeolites. Rewardingly, it appears that an optimum could be found between $0.15-0.25\ cm^3$ / g. Though a partial loss of regular microstructure was observed after hydrothermal treatment either performed with HL or OHL acting as *BSST,* a higher degree of 2 methylphenyl 3-phenylpropynoate conversion could clearly be reached at an optimal mesoporous volume (Fig. 5). No significant change in the selectivity could be detected while changing the mesoporous volume, being around 40–50 % whatever the post-modified FAU catalyst.

It is important to mention that the presence of EFAl Lewis species is neither catalyzing, nor beneficial for the conversion of *O*-aryl ester of 3-arylpropynoic acid. Contrarily, the presence of those species probably hinders the access towards the BrØnsted acid sites, known as real active sites for this acid-catalysed reaction [35]. Indeed, the poor conversion achieved over EFAL-USY sample was doubled after the removal of EFAl species in No-EFAl-USY sample as catalyst (30 vs 14 %). Interestingly, similar selectivity could be achieved while removing those EFAl species in No-EFAl-USY, which contains roughly 1.5 times less acid sites. It seems therefore that the presence of BrØnsted acid sites is a necessary condition but not sufficient to perform this reaction at high conversion and selectivity. Indeed, it was recently shown that BrØnsted acidity or even superacidity (CF_3SO_3H, triflic acid, H_o = -14.1) alone was not sufficient to selectively afford targeted coumarin compounds [35].

These catalytic data suggest that efficient cyclization reaction occurred at the acid sites present within the micropores, as shown by the good selectivity achieved over pristine H–Y, but that a certain degree of mesoporosity is required to reach these micropores (compared A4 with H–Y). Due to the size of the starting ester and more importantly of the coumarin products (7–8 and $8-10$ Å diameter, respectively), diffusion could be limited [35,36]. Alternatively, with a highly modified and altered zeolite such as A13, less acidic sites may be available despite a Si/Al ratio of 15, and with a Emmenthal cheese-like structure, compounds may just diffuse through, without much interactions with the catalyst surfaces.

4. Conclusion

In this study, the effect of various treatments subjected to FAU zeolite crystals to introduce mesoporosity has been examined on their efficiency as catalyst for the cyclisation of *O*-aryl 3-arylpropynoic acid ester to corresponding coumarin.

Desilication while adding lignin residues, but for a limited time, offered the best combination regarding conversion and selectivity,

Table 3
FAU catalysts performance in the conversion of 2-methylphenyl 3-phenylpropynoate into its corresponding 8-methyl-4-phenyl-*2H*-chromen-2-one coumarin.

Catalyst	Conversion of 2 methylphenyl 3-phenylpropynoate [%]	Selectivity in 8-methyl-4-phenyl-*2H*-chromen-2-one [%]
HY	30	60
EFAl-HUSY	14	36
No-EFAl-HUSY	30	47
D14	47	43
A4	56	52
A13	18	39

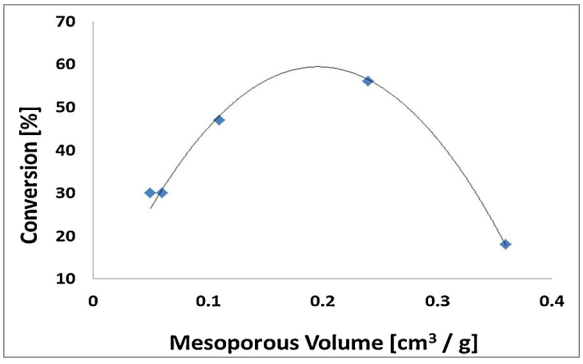

Fig. 5. Conversion of 2-methylphenyl 3-phenylpropynoate as a function of the zeolite mesoporous volume.

confirming the so-called bio-sourced secondary template (BSST) concept in the design of zeolite-based catalysts.

The catalytic data gained from this study revealed that a certain degree of mesoporosity is needed and that an optimum could be found for the conversion of these esters into coumarins.

This zeolite-promoted cyclization of aryl propynoate provides a rapid and mild access to coumarins, thus conforting zeolites as a key player in green organic synthesis.

Credit author statement

B. Louis, P. Pale, V. Beneteau and A.V. Vasiliev, Conceptualization, methodology and validation

E.I. Evstigneyev, S. Shanmugam, Formal analysis and characterisation

O. Zaitceva, Investigation, doing experiments

B. Louis, A.V. Vasiliev, P. Pale writing – original draft

V. Beneteau, P. Pale, B. Louis, A.V. Vasiliev, Supervision

Declaration of Competing Interest

The authors declare that they have no known competing financial interests or personal relationships that could have appeared to influence the work reported in this paper.

Acknowledgements

The authors thank the CNRS, the French Ministry of Research and the Estonia – Russia Cross Border Cooperation Program 2014-2020, project number is ER30 (BioStyrene). OZ thanks the Russian Science Foundation for her PhD fellowship.

References

[1] A. Dyer, Encyclopedia of Materials: Science and Technology, (2001).
[2] M. Milina, S. Mitchell, N.L. Michels, J. Kenvin, J. Perez-Ramirez, J. Catal. 308 (2013) 398.
[3] L. Tosheva, V. Valtchev, Chem. Mater. 17 (2005) 2494.
[4] J. Jiang, J. Yu, A. Corma, Angew. Chemie Int. Ed. 49 (2010) 3120.
[5] J.L. Paillaud, B. Harbuzaru, Science 304 (2004) 990.
[6] J. Kim, M. Choi, R. Ryoo, J. Catal. 269 (2010) 219.
[7] J.C. Groen, W. Zhu, S. Brouwer, S.J. Huynink, F. Kapteijn, J.A. Moulijn, J. Pérez-Ramírez, J. Am. Chem. Soc. 129 (2007) 355.
[8] S. van Donk, A.H. Janssen, J.H. Bitter, K.P. de Jong, Catal. Rev. 45 (2003) 297.
[9] D. Verboekend, J. Pérez-Ramírez, Catal. Sci. Technol. 1 (2011) 879.
[10] A. Astafan, M.A. Benghalem, Y. Pouilloux, J. Patarin, N. Bats, C. Bouchy, T.J. Daou, L. Pinard, J. Catal. 336 (2016) 1.
[11] A.I. Lupulescu, J.D. Rimer, Angew. Chem. Int. Ed. 51 (2012) 3345.
[12] M. Maldonado, M.D. Oleksiak, S. Chinta, J.D. Rimer, J. Am. Chem. Soc. 135 (2013) 2641.
[13] A.I. Lupulescu, M. Kumar, J.D. Rimer, J. Am. Chem. Soc. 135 (2013) 6608.
[14] J.D. Rimer, R.F. Lobo, D.G. Vlachos, Langmuir 21 (2005) 8960.
[15] B. Louis, E.S. Gomes, P. Losch, G. Lutzweiler, T. Coelho, A. Faro Jr., J.F. Pinto, C.S. Cardoso, A.V. Silva, M.M. Pereira, ChemCatChem 9 (2017) 2065.
[16] E.S. Gomes, G. Lutzweiler, P. Losch, A.V. Silva, C. Bernardon, K. Parkhomenko, M.M. Pereira, B. Louis, Microporous Mesoporous Mater. 254 (2017) 28.
[17] R. Bingre, C.M. Sayago, P. Losch, L. Huang, Q. Wang, M.M. Pereira, B. Louis, Inorganica Chim. Acta 487 (2019) 379.
[18] M.M. Pereira, E.S. Gomes, A.V. Silva, A.B. Pinar, M.G. Willinger, S. Shanmugam, C. Chizallet, G. Laugel, P. Losch, B. Louis, Chem. Sci. 9 (2018) 6532.
[19] B. Louis, E.S. Gomes, T. Coelho, G. Lutzweiler, P. Losch, A.V. Silva, A.C. Faro Jr., T. Romero, M. Ben Osman, A. Balanqueux, C. Bernardon, M.M. Pereira, Nanosci.Nanotechnol. Lett. 8 (2016) 917.
[20] C.C. Rocha, A. Balanqueux, M. Boltz, P. Losch, C. Bernardon, V. Bénéteau, P. Pale, M.M. Pereira, B. Louis, L'Act. Chim. (2015) 393–394.
[21] J. Perez-Ramírez, C.H. Christensen, K. Egeblad, C.H. Christensen, J.C. Groen, Chem. Soc. Rev. 37 (2008) 2530.
[22] F. Thibault-Starzyk, I. Stan, S. Abelló, A. Bonilla, K. Thomas, C. Fernandez, J.P. Gilson, J. Pérez-Ramírez, J. Catal. 264 (2009) 11.
[23] M.L. Rabinovich, Wood hydrolysis industry in the Soviet Union and Russia: what can be learned from history? Proceedings of NWBC2009, Helsinki, Finland, September 2–4 (Rautakivi, A., Ed.), 2020, pp. 111–120.
[24] E.I. Evstigneyev, O.S. Yuzikhin, A.A. Gurinov, A.Y. Ivanov, T.O. Artamonova, M.A. Khodorkovskiy, E.A. Bessonova, A.V. Vasilyev, J. Wood Chem. Technol. 36 (2016) 259.
[25] C.W. Dence, The determination of lignin, in: S.Y. Lin, C.W. Dence (Eds.), Methods in Lignin Chemistry, Springer-Verlag, Berlin, 1992, pp. 33–61.
[26] E.I. Evstigneyev, Russian J. Bioorg. Chem. 43 (2017) 732.
[27] G.F. Zakis, Functional Analysis of Ligninsand Their Derivatives, TAPPI Press, Atlanta, GA, 1994.
[28] K. Wilson, Determination of carboxylgroups in cellulose, Svensk. Papperstidn. 51 (1948) 45.
[29] E.I. Evstigneyev, Russian J. Appl. Chem. 86 (2013) 258.
[30] P. Mänsson, Holzforschung 37 (1983) 143.
[31] J.A. van Bokhoven, A.L. Roest, D.C. Koningsberger, J.T. Miller, G.H. Nachtegaal, A.P.M. Kentgens, J. Phys. Chem. B 104 (2000) 6743.
[32] P. Losch, T.C. Hoff, J.F. Kolb, C. Bernardon, J.P. Tessonnier, B. Louis, Catalysts 7 (2017) 225.
[33] R. Bingre, P. Losch, C.M. Sayago, B. Vincent, P. Pale, P. Nguyen, B. Louis, ChemPhysChem 20 (2019) 2874.
[34] (a) F. Borges, F. Roleira, N. Milhazes, L. Santana, E. Uriarte, Curr. Med. Chem. 12 (2005) 887;
(b) S. Penta, Advances in Structure Activity Relationships of Coumarin Derivatives, Academic Press, Oxford, 2016;
(c) A. Stefanachi, F. Leonetti, L. Pisani, M. Catto, A. Carotti, Molecules (23) (2018) 250.
[35] O. Zaitceva, V. Beneteau, D.S. Ryabukhin, B. Louis, A.V. Vasilyev, P. Pale, ChemCatChem 12 (2020) 326–333.
[36] P. Losch, J.F. Kolb, A. Astafan, T.J. Daou, L. Pinard, P. Pale, B. Louis, Green Chem. 18 (2016) 4714.